Efficient Radiation Production in Long Implosions of Structured Gas-Puff *Z* Pinch Loads from Large Initial Radius

H. Sze,[1] J. Banister,[1] B. H. Failor,[1] J. S. Levine,[1] N. Qi,[1] A. L. Velikovich,[2] J. Davis,[2] D. Lojewski,[3] and P. Sincerny[1]

[1]*L-3 Titan Pulse Sciences Division, San Leandro, California, 94577, USA*

[2]*Plasma Physics Division, Naval Research Laboratory, Washington, D.C. 20375, USA*

[3]*Defense Threat Reduction Agency, Albuquerque, New Mexico 87117, USA*

(Received 2 May 2005; published 1 September 2005)

We have proposed and demonstrated successfully a new approach for generating high-yield *K*-shell radiation with large-diameter gas-puff *Z* pinches. The novel load design consists of an outer region plasma that carries the current and couples energy from the driver, an inner region plasma that stabilizes the implosion, and a high-density center jet plasma that radiates. It increased the Ar *K*-shell yield at 3.46 MA in 200 ns implosions from 12 cm initial diameter by a factor of 2, to 21 kJ, matching the yields obtained earlier on the same accelerator with 100 ns implosions. A new ''pusher-stabilizer-radiator'' physical model is advanced to explain this result.

DOI: 10.1103/PhysRevLett.95.105001 PACS numbers: 52.59.Px, 52.35.Py, 52.58.Lq

Dense *Z* pinch plasmas are the most powerful and energy-efficient laboratory sources of x rays in the photon energy range from hundreds of eV to several keV. Record high radiation yields (~1.8 MJ in soft x rays [1], ~400 kJ in Al, and ~300 kJ in Ar *K*-shell emission, at 1.7 and 3 keV, respectively [2,3]), have recently been obtained on the *Z* accelerator at Sandia with tungsten and aluminum nested wire arrays and argon double-shell gas puffs driven by 15–20 MA, 100 ns current pulses. These successes are promising for inertial confinement fusion and other applications, such as 10–20 keV x-ray production, on next-generation *Z* pinch drivers, from *ZR* (26 to 30 MA, 100 to 300 ns) [4] in the near term, to 40–60 MA machines of the future.

This broad research area will advance considerably if we find a way to efficiently produce x rays with *Z* pinch loads imploded by slower-rising current pulses, 200–300 ns or longer. Interest in longer current pulses is stimulated both by the restrictions on the voltage applied to the front end of the driver, $V \propto I_m/\tau$ (here, I_m is the peak current and τ is its rise time), and by the substantial cost reductions offered by slower pulsed power [5]. Larger initial load radii, R_0, have been thought to be needed for matching the loads to slower drivers, as well as for accelerating the imploded loads to higher velocity, v, necessary to generate harder *K*-shell and/or free-bound [6] radiation. To efficiently produce *K*-shell emission, kinetic energy per ion in an annular load must exceed the threshold energy E_I needed to strip the ion down to the He-like state by a factor of $\eta = m_i v^2/2E_I$, whose value should be at least ~2, and better between 3 and 5 (where m_i is the ion mass).

The major problem of implosions from large radii is the Rayleigh-Taylor (RT) instability of accelerated plasma. A longer acceleration path amplifies the RT instability growth. In addition, for a fixed load mass μ that provides the desired value of η at given I_m, a constant compression ratio implies $Y_K \sim 1/R_0 \sim 1/\tau$. If this scaling, supported by some experimental data [7], always holds, the long implosions would be inherently inferior to the short implosions. To increase the initial radius of the load without sacrificing its radiative performance, we have to improve, rather than maintain, the quality of its implosion. We have to increase the compression ratio and axial uniformity of the pinch and enhance the energy coupling to the stagnated radiating plasma. While conventional wisdom [7] indicates that this is hardly possible, the purpose of this Letter is to demonstrate how it can be done.

Our strategy is to suppress the RT instability of implosion by shaping the peripheral load density profiles as described in [8–12] and at the same time to separate the dual role of the plasma in a conventional *Z* pinch that requires it to both couple energy during the run-in phase and then radiate at high η [13] at implosion. The role of the outer region plasma (''pusher'') is to carry current during the rise time of the current drive and push as it implodes. It does not need to mix with the inner region and center plasma and be heated for efficient *K*-shell radiation. The inner plasma (''stabilizer'') shapes the mass distribution with density gradient directed toward the pinch axis, which, according to theory and simulations [9], mitigates the RT instability of implosion. The dense center jet plasma serves as a ''radiator.'' It is first preheated by a converging shock wave when the imploding plasma approaches the axis, and is then heated quasiadiabatically as long as the implosion continues [13]. A large fraction of the total energy coupled to the plasma is converted to the thermal energy of the radiator, and the proper choice of the center jet mass ensures that the optimal conditions for radiation are produced, i.e., a sufficiently high electron temperature (1.5 to 2 keV for Ar *K*-shell emission) and the largest mass at the highest density compatible with it.

We report the experiments conducted on a ~3.5 MA generator operating in a ~200 ns long-pulse mode. The argon gas-puff load is injected by the 12 cm diameter nozzle recently developed [8] to match the 300 ns rise time of a new generation of longer rise time pulsed-power

generators. The nozzle has two recessed annuli and a very high mass center jet; see Fig. 1(a). The inner and outer annuli span from 2 to 3 cm and from 5 to 6 cm in radius, respectively; the jet is 0.5 cm in radius, on axis.

By selectively filling the two shells and the center jet with argon, we tested four mass profiles: (1) inner and outer shell (inner-outer), as in [3,8,14]; (2) center jet and outer shell (jet-outer); (3) center jet and inner shell (jet-inner) [15]; (4) center jet and both shells (jet-inner-outer). We use a planar laser-induced fluorescence technique to map the time-resolved absolute cold gas density profile in the radial and axial directions [11]. The distributions of mass density and mass density times radius (illustrating that much of the load mass is where its density is relatively low) at the pinch midplane of the four different loads are shown in Fig. 1(b).

We use a Rogowski coil to measure current in the load, filtered calorimeters and filtered x-ray diodes (XRDs) to measure the K-shell yield and radiation pulse shape, time-resolved x-ray PIN diodes to look at time history of the K-shell radiation spatially resolved along the axis, a CCD-based time-integrated x-ray pinhole camera to look at the K-shell pinch uniformity and radius, and a CCD-based spectrometer to measure the spectrum. All K-shell x-ray diagnostics viewed the entire 3.8 cm length of the pinch from cathode to anode. In addition, an extreme ultraviolet (XUV) spectrometer recorded emission averaged over a 2 mm axial length of the pinch at a distance of 1 cm from the cathode. The 12 current return posts are located at 7.8 cm radius. UV flashboards are used to provide ionization before the current drive.

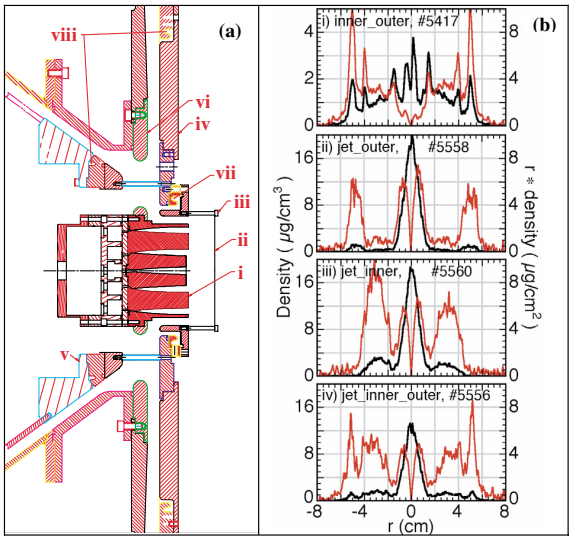

FIG. 1 (color). (a) Experimental setup. (i) Nozzle, (ii) pinch anode plane, (iii) current return posts, (iv) lower anode, (v) upper anode, (vi) cathode, (vii) load Rogowski, and (viii) MITL Rogowskis. (b) Gas mass density (black) and radius times mass density (red) distributions at midplane of a 3.8 cm-long puff for four mass profiles indicated.

A chlorine tracer was introduced in the form of freon12 (CF_2Cl_2), 2% by partial pressure, to trace the origin of the K-shell radiation. The jet-inner-outer profile was tested 3 times for reproducibility and to allow chlorine tracing in the center jet, inner shell, and outer shell, respectively. Each of the jet-inner, jet-outer, and inner-outer profiles were tested 2 times for reproducibility and the chlorine tracer test. For all 9 shots, the total injected mass, the peak current, and the implosion time ranged from 104 to 140 μg/cm, from 3.37 to 3.57 MA, and from 200 to 210 ns, respectively.

Figure 2 shows the current drive waveforms and the K-shell radiation pulse shapes for each of the four mass profiles. Figure 3 presents the records of a linear array of 14 PIN diodes looking at the 3.8 cm-long pinch through a slit with each diode limited to viewing about 3 mm in the axial direction, filtered so that its response is dominated by the continuum at photon energies greater than the K-shell lines. The contours shown in Fig. 3 provide the time history and axial radiation profile from the cathode to the anode. Figure 3 also shows images of the time-integrated K-shell radiation and pinch radii of the four mass profiles along the 3.8 cm pinch. The experimental results are summarized in Table I.

For the inner-outer profile, the implosion produces a radiation pulse that is narrow, 5.5 ns FWHM [Fig. 2(a)], and a radiating plasma of ~1.5 mm radius that is both uniform and straight [Fig. 3(a)]. The argon K-shell yield is ~10 kJ, which represents an optimization of total load mass μ and the mass ratio μ_{in}/μ_{out} carried out over more than 30 tests with this profile on this accelerator. This is a significant reduction from the yields that were produced in other ~3.5 MA argon Z pinch experiments at

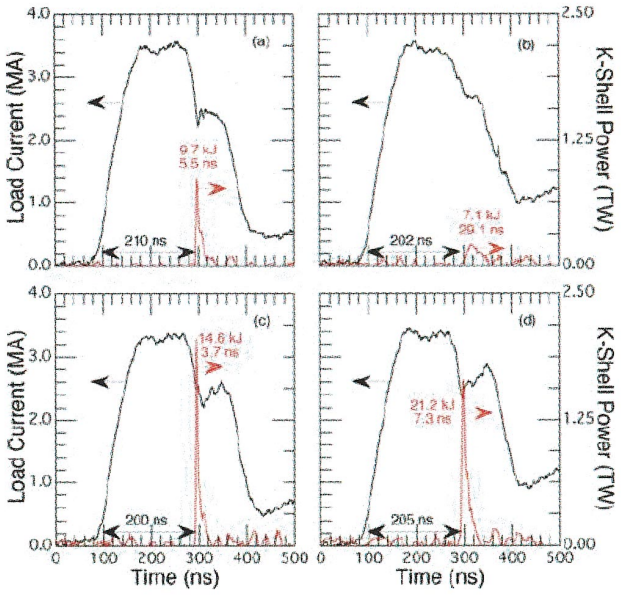

FIG. 2 (color). Current and K-shell power waveforms for four different mass profiles: (a) inner-outer, (b) jet-outer, (c) jet-inner, and (d) jet-inner-outer.

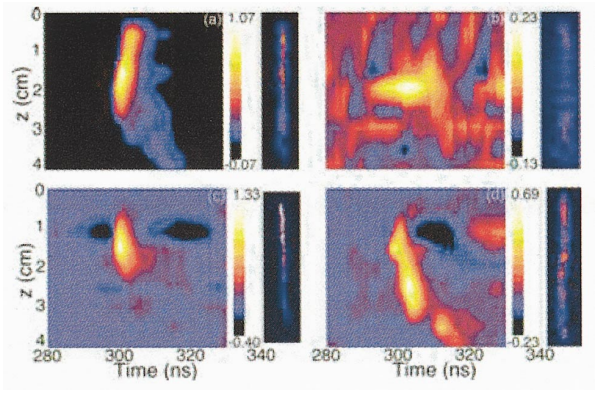

FIG. 3 (color). Length (relative to the cathode) vs time contours of the x-ray intensity (K-shell and above) and the time-integrated pinhole camera image for four different mass profiles. (a) Inner-outer, (b) jet-outer, (c) jet-inner, and (d) jet-inner-outer. Each pinhole picture is independently scaled for intensity vs color. For the length vs time intensity contours, the signal levels indicated by the color bars can be compared numerically, though (a) had reduced filtration with respect to the other profiles by 25.4 μm of Al.

shorter implosion times or smaller initial radii: (1) for a 100 ns implosion time, 20 kJ has been obtained using a 2.5 cm diameter, single-shell nozzle [16] and (2) for a 200 ns implosion time, 16 kJ was achieved with an 8 cm double-shell nozzle [14]. Based on this result, one would be tempted to conclude that the current database adds credibility to the pessimistic scaling $Y_K \sim 1/R_0$. We will demonstrate below how misleading such a conclusion is.

The three other profiles, tested to determine their stability and radiation generation efficiency, included a massive center jet and differed by the inclusion, or exclusion, of either the inner or outer shells. For the jet-outer profile, this is a thin large-diameter (12 cm) annular shell with an extended low density region separating it from the center jet. This load produced only a 7 kJ K-shell yield. A broad, multispike, 29 ns K-shell pulse, low peak power [Fig. 2(b)], and the absence of well-localized x-ray intensity contours confirm that its implosion is distorted by the RT instability and fails to produce a tight pinch at stagnation, as seen in the pinhole photograph of Fig. 3(b).

For the jet-inner profile, the current-carrying peripheral part is a diffuse 6 cm diameter shell, contiguous to the center jet, whose implosion must be much less affected by the RT instability than the 12 cm shell. Indeed, this load performs very well, generating a 15 kJ K-shell yield in a short 3.7 ns pulse [Fig. 2(c)], and the highest K-shell power (XRD pulse shape normalized to calorimeter yield) of about 2.05 TW. The stagnated pinch is the narrowest of all [Fig. 3(c)], but not uniform from cathode to anode; the radiating zone is highly localized at 1–2 cm from the cathode. Note the low penalty paid for the apparent mismatch between the small initial diameter of the load (6 cm) and the long implosion time (200 ns), which is conventionally thought to translate into small η. The current through this load can be increased if its inductance was decreased by placing the return current posts closer to the axis. Scaling 15 kJ at 3.37 MA up to 3.6 MA, we predict that this load can generate $\sim$18 kJ. Therefore, it produces K-shell x rays as well as or better than the 8 cm diameter nozzle at 3.6 MA, which supports the "pusher-radiator" arguments of [13].

The jet-inner-outer profile features the same peripheral density distribution as the inner-outer [Fig. 1(b)], with the presence of the inner shell stabilizing the implosion of the outer shell [9]. Until the imploding plasma reaches the center jet, its implosion must be as stable as that of the inner-outer. Indeed, the radiation pulse widths that characterize the tightness of stagnated pinch are close for these two cases, 5.5 and 7.3 ns. The K-shell yield produced by the jet-inner-outer profile, however, is 21 kJ—twice as high as for the inner-outer profile, greater than the yields obtained with the 8 cm diameter double-shell load at 200 ns implosion [14], the same as produced with a 2.5 cm diameter single-shell load at 100 ns [16]. The stagnated pinch is straight and uniform, with a narrow radiating zone extending from 1 to 3 cm from the cathode [Fig. 3(d)]. This result is also robust, having been reproduced in all three shots with this configuration, and can only be improved by further optimization. Apparently, it is the presence of the dense center jet that makes the difference here.

The center jet plasma is too close to the axis to gain a high velocity before stagnation. It is heated by the shock wave produced when the imploding outer plasma hits the center jet, and then adiabatically, as the stagnated plasma continues to converge. Simulations [13] predict a long prepulse of sub-keV radiation to emerge as the density of the jet is increased, a key signature that indicates the shock

TABLE I. Comparison of mass, implosion, and radiation results for four different mass profiles. τ_K is the FWHM of the K-shell radiation pulse, and Y_K and W_K are the K-shell yield and peak power, respectively. Electron temperature T_e is energy weighted and axially averaged.

Profile and shot No.	μ (μg/cm)	I_m (MA)	τ_K (ns)	Y_K (kJ)	W_K (TW)	T_e (keV)
Inner-Outer 5417	120	3.57	5.5	9.7	0.87	1.69
Jet-Outer 5558	104	3.57	29.1	7.1	0.22	1.24
Jet-Inner 5560	140	3.37	3.7	14.6	2.05	1.45
Jet-Inner-Outer 5556	135	3.46	7.3	21.2	1.65	1.64
Estimated $\pm$ uncertainties	10%	0.2	1	10%	10%	10%

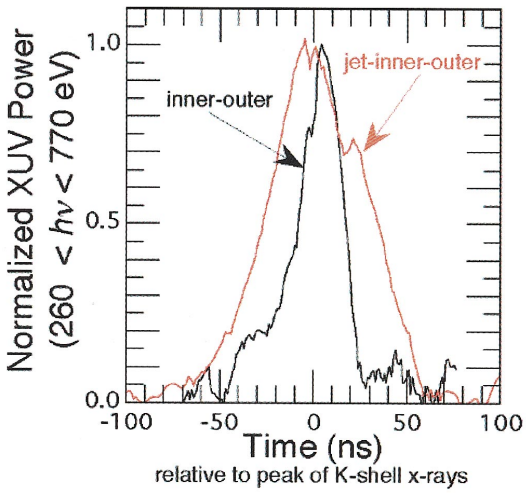

FIG. 4 (color). Comparison of XUV emission produced by jet-inner-outer and inner-outer gas profiles. Trace peaks are normalized to unity to emphasize differences in shape and timing. Shots with a high mass jet have a long, relatively gentle rise time compared to shots without a jet.

wave is passing into the on-axis plasma. As shown in Fig. 4, such a prepulse in the XUV spectral range ($260 < h\nu < 770$ eV), ~20 ns earlier relative to the K-shell radiation peak than in the inner-outer case, is indeed observed; also, the relatively slow emission rise time is characteristic of a quasiadiabatic, or reversible, compression. In the inner-outer case, the rise time is much more rapid with a sharp jump (characteristic of a rapid, irreversible compression) at the time of peak K-shell emission. Thus, by adding a massive center jet, the dynamics of the implosion are changed dramatically and the compression and temperature increase of the plasma become much more adiabatic.

To prove that the center jet plasma is indeed the radiator, we trace the origin of the radiation. Since each shell and jet has its own plenum, it is possible to identify the radiation from each by the use of a chlorine tracer introduced into a single plenum. For the jet-inner-outer profile tests, we rotated the tracer in each shell and jet in a 3-shot series. Looking at the relative Cl excitation efficiency (defined as the ratio of the Cl signal to the Ar K-line signal), we estimate that about 65% of the 21 kJ K-shell radiation is produced by the center jet plasma, while the remaining 30% and 5% are from the inner and outer shell plasmas, respectively. For the jet-inner profile, 75% of the 15 kJ comes from the center jet plasma and 25% from the inner shell plasma. For the jet-outer profile test, >95% of the 7 kJ is from the jet. For the inner-outer profile, 95% of the 10 kJ comes from the inner shell and the remaining 5% comes from the outer shell.

To summarize, we have successfully demonstrated how the imploding and radiating components of a gas-puff load can be, and should be, designed and optimized separately for their respective roles. This finding opens a new parameter space for load design and new opportunities for Z pinch experiments. The "pusher-stabilizer-radiator" concept is not limited to long-pulse drivers and large radius loads. It can be extended to improve the quality of implosions driven by short current pulses to further optimize radiation production. This suggests that either the conventional wisdom of decreased yield with larger diameter and long implosion Z pinches has been overturned, or this new approach can lead us to even higher yields in short (~100 ns) implosions with new smaller-diameter (5 to 8 cm) nozzles, e.g., exceeding the 300 kJ Ar obtained with a 8 cm diameter double-shell nozzle at 15 MA [3]. The jet-inner profile demonstrated that in implosions driven by slower current pulses the pusher does not necessarily have to start from a larger radius, $R_0 \propto \eta^{1/2}\tau(\hbar\omega)^{2/3}$, to maintain high η; rather, the pusher can rapidly deliver the required thermal energy to the radiator via shock and quasiadiabatic compression, effectively amplifying η in the radiator, as in our jet-inner case.

The authors are grateful to J. Riordan, L. I. Rudakov, P. Steen, J. W. Thornhill, K. G. Whitney, and A. Wilson for useful discussions. This work was sponsored by the Defense Threat Reduction Agency. The authors are also grateful to all the other participants of the DTRA-sponsored research program for their contributions that made our present progress possible.

[1] C. Deeney *et al.*, Phys. Rev. Lett. **81**, 4883 (1998).
[2] C. A. Coverdale *et al.*, Bull. Am. Phys. Soc. **48**, No. 7, 237 (2003).
[3] H. Sze *et al.*, Phys. Plasmas **8**, 3135 (2001).
[4] D. H. McDaniel *et al.*, in *Dense Z-Pinches*, edited by J. Davis, C. Deeney, and N. R. Pereira, AIP Conf. Proc. No. 651 (AIP, New York, 2002), p. 23.
[5] K. Ware *et al.*, IEEE Trans. Plasma Sci. **28**, 1397 (2000); E. A. Azizov *et al.*, in *Dense Z-Pinches*, edited by J. Davis, C. Deeney, and N. R. Pereira, AIP Conf. Proc. No. 651 (AIP, New York, 2002), p. 29; P. Spence *et al.*, *ibid.*, p. 43.
[6] A. L. Velikovich *et al.*, Phys. Plasmas **8**, 4509 (2001).
[7] K. D. Ware *et al.*, IEEE Trans. Plasma Sci. **30**, 1733 (2002).
[8] J. S. Levine *et al.*, Phys. Plasmas **11**, 2054 (2004).
[9] A. L. Velikovich *et al.*, Phys. Rev. Lett. **77**, 853 (1996); Phys. Plasmas **5**, 3377 (1998).
[10] T. W. L. Sanford *et al.*, in *Conference Record-Abstracts, 23rd IEEE International Conference on Plasma Science* (IEEE, New York, 1996), p. 251; J. S. Levine *et al.*, Phys. Plasmas **8**, 533 (2001).
[11] B. H. Failor *et al.*, Rev. Sci. Instrum. **74**, 1070 (2003).
[12] N. Qi *et al.*, IEEE Trans. Plasma Sci. **33**, 752 (2005).
[13] L. I. Rudakov *et al.*, Bull. Am. Phys. Soc. **48**, No. 7, 239 (2003); A. S. Chuvatin *et al.*, IEEE Trans. Plasma Sci. **33**, 739 (2005).
[14] H. Sze *et al.*, Phys. Plasmas **7**, 4223 (2000).
[15] T.-F. Chang *et al.*, J. Appl. Phys. **69**, 3447 (1991).
[16] C. Deeney *et al.*, J. Appl. Phys. **75**, 2781 (1994).